New Nonionic Head Type Polysoaps: A Way to Reversed Liquid Crystalline Phases

Claudius Schwarzwälder and Wolfgang Meier*

Institut für Physikalische Chemie Universität Basel, Klingelbergstrasse 80, CH-4056 Basel, Switzerland

Received March 25, 1997; Revised Manuscript Received June 3, 1997[⊗]

ABSTRACT: The preparation and characterization of new oligooxyethylene alkyl ether surfactants and their corresponding polysoaps are described. The monomers are epoxy-terminated at their hydrophilic end, which allows an $AcAc/H_2O/AlEt_3$ catalyzed polymerization to high molecular weight polymers with a water-soluble backbone. The behavior of the monomers and polymers in water and organic solvents is characterized by static and dynamic light scattering. The binary phase diagrams of these surfactants with water display broad lyotropic liquid crystalline phases. The identical chemical constitution of the polymeric backbone and the hydrophilic head groups of the surfactant units enables the formation of reversed aggregates. As a consequence, for the first time, a reversed hexagonal phase in side-chain polymeric surfactants is observed.

Introduction

Due to their amphiphilic character surfactants are able to build up self-assembled structures in polar as well as in apolar media. At low concentrations usually the formation of micelles with spherical, rodlike, or disclike shape occurs. These micelles, again, can aggregate to lyotropic liquid crystalline phases at higher concentration.

Interconnecting of individual surfactant molecules via chemical bonds leads to polymeric surfactants. The superstructures of these polymers show often a considerable stabilization, due to a restricted mobility of the individual subunits.[1] Their aggregation behavior has recently been described theoretically.[2]

Polymeric surfactants have found increasing attention, e.g., as model systems for more complex biologically relevant macromolecules or for a multitude of industrial, pharmaceutical, or cosmetic applications.[3]

The incorporation of monomeric surfactants into side-chain polymers can be realized by polymerization at their hydrophilic headgroup, their hydrophobic tails, or even or their hydrophilic−hydrophobic boundary. An introduction and review about these systems was recently published.[4]

The type of the attachment has considerable influence on the phase behavior of aqueous polymer solutions.[5] Sterical constraints should force tail-type polysoaps to form exclusively normal micellar aggregates and liquid crystalline phases. The opposite, the formation of inverse mesophases, is expected for the head-type. Hitherto this could, however, not be experimentally verified.

The only detailed investigation of the phase behavior of a head-type system, consisting of oligooxyethylene alkyl ether attached to a polyacrylate backbone, found besides a broad miscibility gap only normal and no type of reversed liquid crystalline phases.[6]

While this clearly displays that no suppression of normal aggregates occurs, the question arises why despite the headgroup attachment no reversed liquid crystalline phase was observed.

One possible explanation could be the rather hydrophobic character of the polyacrylate main chain, which is probably not compatible with the polar surrounding within the hydrophilic core of a reversed aggregate.

Consequently, a polymer backbone which is chemically identical to the hydrophilic head of the oligooxyethylene alkyl ether surfactant can be expected to fit much better into such a surrounding and should, therefore, allow for the first time the realization of side chain polymeric amphiphiles with reversed liquid crystalline phases.

In this paper we describe the synthesis and characterization of oligooxyethylene alkyl ether surfactants bearing a polymerizable epoxy group at their hydrophilic end and their corresponding polymers. Properties of the monomers in dilute aqueous solvents and of the polymers in dilute organic solvents are investigated by static and dynamic light scattering.

Polarizing miscroscopy and X-ray diffraction measurements allow the determination of lyotropic mesophases of the monomeric and polymeric surfactants.

Experimental Section

Synthesis. The synthesis up to the oligooxyethylene alkyl ether **3a/b** (see Scheme 1) followed the common path with several steps of williamson ether synthesis and is described in the literature.[7−10] An alternative route via hexaethylene glycol led to difficulties in the purification of the obtained hexaethylene glycol monoalkyl ether.

The polymerizable headgroup of the nonionic surfactant was introduced by further williamson ether synthesis of **3a/b** with allyl bromide followed by epoxidation of the resulting product **4a/b** with 3-chloroperbenzoic acid.[11] The solvent was evaporated and the monomer **5a/b** was dried 12 h in oil vacuum.

Between different polymerizations the individual monomers were stored under Ar atmosphere. Polymerization (Scheme 2) was carried out in bulk under slight argon overpresssure with a acetylacetone/water/$AlEt_3$ catalyst known to be able to produce high molecular weight polymers from epoxides.[12−14] Similar catalyst systems like dmg/Ni/$AlEt_3$ which were used to polymerize, e.g., octadecylethylene oxide,[15] failed with our monomers. Anionic polymerization using sodium naphtalide or potassium alcoholates produced only oligomers with a degree of polymerization between three and five.

Synthesis of 4a/b (4,7,10,13,16,19,22-Heptaoxadotricont-1-ene/4,7,10,13,16,19,22-Heptaoxatetratricont-1-ene). A mixture of 230 g (0.54 mol) of **3a** was placed under inert atmosphere in a carefully dried 1-L three-necked flask and dissolved in 400 mL of absolute 1.4-dioxane. After addition of 12.4 g (0.54 mol) of sodium the mixture was slowly heated up to 110 °C and stirred until all the sodium had

[⊗] Abstract published in *Advance ACS Abstracts,* July 15, 1997.

S0024-9297(97)00410-5 CCC: $14.00

Scheme 1. Synthesis of Epoxy-Terminated Oligooxyethylene Alkyl Ether Monomers

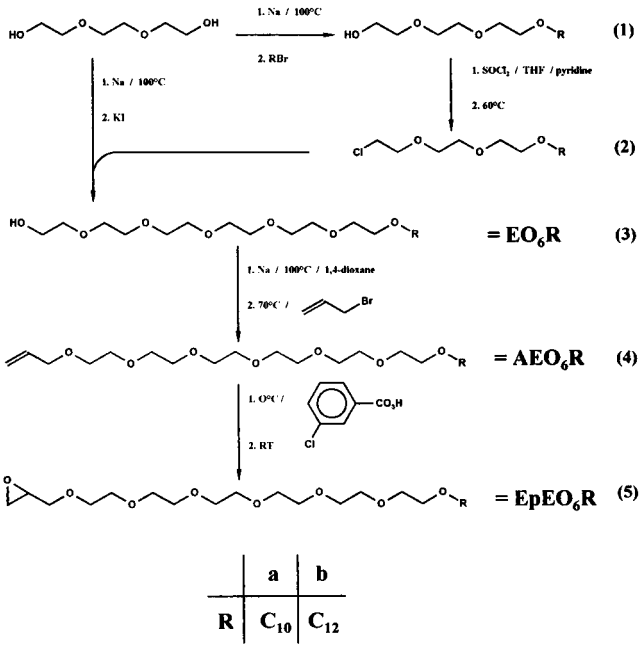

reacted. Subsequently 51 mL (0.6 mol) of allyl bromide were dropped in at 70 °C and the reaction mixture was stirred for another 6 h. The mixture was poured in water and extracted several times with petroleum ether (boiling range 30−70 °C). The remaining organic phase was dried over magnesium sulfate. The solvent was removed and the remaining oil was distilled.

The product **4a** was obtained at 220 °C/1.3 × 10^{-2} mbar. A thin layer chromatography analysis showed the educt **3a** as the only impurity.

Flash chromatography with a mixture of acetone/petroleum ether (boiling range 35−70 °C) 1:2 as solvent gave a clear colorless oil of 160 g (0.35 mol) pure product **4a** (yield 65%; GC purity, 98%).

^{1}H NMR ($CDCl_3$/TMS) δ (ppm): 5.9 (m, 1 H), 5.3 (d, 1 H), 5.2 (d, 1 H), 4.0 (d, 2 H), 3.7−3.4 (m, 26 H), 1.6 (m, 2 H), 1.3 (m, 14 H), 0.8 (t, 3 H).

4b was synthesized analogously to **4a**. Acetone/petroleum ether 1:1 was used as solvent for flash chromatography (yield 65%; GC purity, 97%).

^{1}H NMR ($CDCl_3$/TMS) δ (ppm): 5.9 (m, 1 H), 5.3 (d, 1 H), 5.2 (d, 1 H), 4.1 (d, 2 H), 3.7−3.4 (m, 26 H), 1.6 (m, 2 H), 1.3 (m, 18 H), 0.8 (t, 3 H)

Synthesis of 5a/b (1,2-Epoxy-4,7,10,13,16,19,22-heptaoxadotricontane/1,2-Epoxy-4,7,10,13,16,19,22-heptaoxatetratricontane). A solution of 151 g (0.32 mol) of **4a** in 700 mL of dichloromethane was placed in a 1-L three-necked flask under inert atmosphere and cooled to 0 °C in an ice bath. Afterwards 78 g (0.33 mol; 70% activity) of *m*-chloroperbenzoic acid was added in small portions under vigorous stirring. After 30 min the reaction mixture was allowed to warm up to room temperature and stirred for another 36 h.

Now the solution was washed three times with 10% sodium sulfite solution until KI starch paper indicated the absence of peroxides. The solution was extracted with 5% sodium hydrogen carbonate solution, water, and finally saturated NaCl. The organic solution was dried ($MgSO_4$) and the solvent was evaporated. The crude product was purified by flash chromatography with a mixture of acetone/petroleum ether 2:3 as solvent. The remaining liquid was dried at room temperature to constant weight. 103 g (0.21 mol) liquid colorless product 5a, was obtained (66% yield; GC purity, 99%) and stored under a slight Ar overpressure in a glass tube at room temperature.

^{1}H NMR ($CDCl_3$/TMS) δ (ppm): 3.8−3.4 (m, 28 H), 3.2 (m, 1 H), 2.8 (m, 1 H), 2.6 (m, 1 H), 1.6 (m, 2 H), 1.3 (m, 14 H), 0.9 (t, 3 H). Calcd: C, 62.73; H, 10.53; O, 26.74. Exptl: C, 62.56; H, 10.38; O, 27.23.

5b was synthesized analogously to 5a using acetone/petroleum ether 8:13 as solvent for flash chromatography (yield 65%; GC purity, 99%).

^{1}H NMR ($CDCl_3$/TMS) δ (ppm): 3.8−3.4 (m, 28 H), 3.2 (m, 1 H), 2.8 (m, 1 H), 2.6 (m, 1 H), 1.6 (m, 2 H), 1.3 (m, 14 H), 0.9 (t, 3 H). Calcd: C, 64.00; H, 10.74; O, 25.26. Exptl: C, 63.86; H, 10.85; O, 25.51.

Initiator. A 25-mL three-necked flask fitted with an Ar inlet, a condenser with an outlet, and a rubber septum was evacuated and carefully dried. A triethylaluminium solution in heptane (Fluka), 15 mL (10 mmol), was injected under argon atmosphere via a syringe. The tube was cooled with an ice−water bath (5 °C) and 1 mL (9.7 mmol) of freshly distilled acetylacetone was added dropwise with a gas-tight argon-purged syringe under a continuous counterflow of argon. The pale yellow solution was stirred for 1.5 h, before 0.09 mL (5 mmol) bidistilled and degassed water was added dropwise. The resulting initiator solution was stirred under a slight argon overpressure for 2 h at room temperature. The solution always consisted of a soluble and an insoluble fraction.[13] This suspension was used for the polymerization.

Polymerization. Polymerization was performed in bulk in a carefully dried glass flask, fitted with PTFE high vacuum taps, under slight Ar overpressure. The flask was flushed with argon, and the monomer was added and heated up to 70 °C. At this temperature the initiator solution (2.5 mol% Al with respect to the monomer) was injected. After polymerization for 48 h (in the case of the high molecular polymer, 2 weeks) the reaction was stopped by injecting a solution of hydrochloric acid in methanol. The polymer precipitated and was washed with acetone. Afterwards the polymers were dissolved three times in dichloromethane and precipitated in methanol. To remove solvent traces the polymers were freeze-dried from benzene. A colorless highly viscous product was obtained.

Three different polysoaps have been synthesized: $PEpEO_6C_{10}$ with a decyl moiety as aliphatic tail and $PEpEO_6C_{12}$ I and $PEpEO_6C_{12}$ II with a longer dodecyl moiety as aliphatic tail. $PEpEO_6C_{12}$ I and -II differ only in their molecular weight (Table 3).

Surface Tension Measurements. The surface tension of defined monomer−water mixtures was determined with a

Scheme 2. Polymerization of Polysoaps with a Polyoxyethylene Backbone

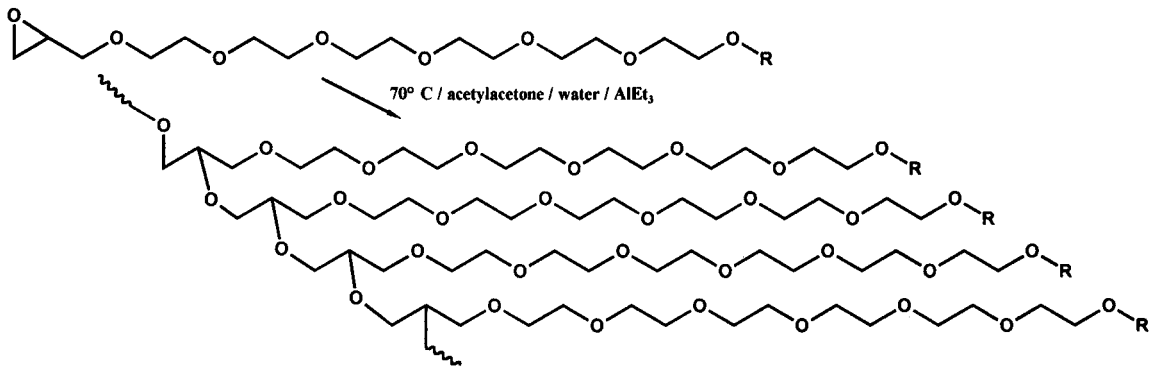

Table 1. Experimental Datas for d*n*/d*c*

substance	solvent	temp, °C	d*n*/d*c*, mL/g
	monomer		
$EpEO_6C_{10}$	water	15	0.1370
$EpEO_6C_{10}$	water	25	0.1331
$EpEO_6C_{10}$	water	35	0.1324
$EpEO_6C_{12}$	water	15	0.1334
$EpEO_6C_{12}$	water	25	0.1328
$EpEO_6C_{12}$	water	35	0.1324
	polymer		
$PEpEO_6C_{10}$	isooctane	25	0.07501
$PEpEO_6C_{10}$	isooctane	45	0.07764
$PEpEO_6C_{12}$	isooctane	25	0.08345
$PEpEO_6C_{12}$	isooctane	45	0.08638
$PEpEO_6C_{12}$	chloroform	25	0.03788

Krüss K8 torsion balance interfacial tensiometer thermostated at 25 °C by using the Du-Noüy-ring method.

The cmc of the monomeric surfactants in water was found to be cmc ($EpEO_6C_{10}$) = 9.9×10^{-4} mol/L and cmc($EpEO_6C_{12}$) = 6.1×10^{-4} mol/L.

Combined Static and Dynamic Light Scattering. The static and dynamic light scattering experiments were performed by using a commercial goniometer (ALV-Langen) equipped with a frequency-doubled NdYAg laser (ADLAS, wavelength $\lambda = 532$ nm) at scattering angles between 30° and 150°. An ALV-5000/E correlator calculates the photon intensity autocorrelation function $g^2(t)$. The samples were prepared by filtering the solutions through a Millipore filter (LCR 0.5 μm) into 10 or 20 mm quartz cells fitted with a Teflon stopper to prevent evaporation of the solvent. The cells were mounted in a thermostated optical matching vat with a temperature accuracy of $T \pm 0.02$ K.

The data of the dynamic light scattering were analyzed by the cumulant method.

The refractive index increment d*n*/d*c* was obtained at the corresponding temperature and wavelength of the light scattering experiments by using a commercial ALV DR-1 differential refractometer. Table 1 shows the data.

Theoretical Background. Static light scattering from dilute solutions is usually described by a virial expansion

$$\frac{Kc}{R(q)} = \frac{1}{M_W P(q)} + 2A_2c + 3A_3c^2 + \dots \quad (1)$$

with the scattering vector $q = (4\pi/\lambda)n_0 \sin(\theta/2)$, where M_W is the weight-average molecular weight, $P(q)$ the particle scattering factor, which can be calculated for many macromolecular structures, and A_2 the second virial coefficient.

The time-averaged scattered light intensity is expressed by $Kc/R(q)$, with an optical contrast factor $K = [(4\pi^2 n_0^2)/(\lambda^4 N_A)](dn/dc)^2$. n_0 is the refractive index of the solvent, c the concentration of the polymer solution, $R(q)$ the Rayleigh ratio of the solution corrected for the contribution of the pure solvent, and d*n*/d*c* the refractive index increment. At small values of q the particle scattering factor can be expanded in a Taylor series, yielding

$$P(q) = 1 - \frac{1}{3}R_G^2 q^2 + \dots \quad (2)$$

with R_G the radius of gyration. Inserting eq 2 in eq 1 yields

$$\frac{Kc}{R(q)} = \frac{1}{M_W}\left(1 + \frac{1}{3}R_G^2 q^2\right) + 2A_2c + 3A_3c^2 + \dots \quad (3)$$

Measurements at finite angle and concentrations can be extrapolated in a Zimm or Berry plot and permit the determination of single particle properties like M_W, R_G, and A_2. Assuming a hard sphere volume interaction, from A_2 a thermodynamically equivalent hard sphere radius R_{HS} can be calculated by using the well-kown relation[16]

$$A_2 = \frac{4N_A V_m}{M_W^2} \quad (4)$$

with

$$V_m = [(4\pi)/3]R_{hs}^3$$

In dynamic light scattering a time correlation function is measured, which is a decaying function in time. From the first cumulant Γ the translatory diffusion coefficient D_c at the concentration c can be determined according to

$$\lim_{q\to 0} \frac{\Gamma}{q^2} = D_c(q) \quad (5)$$

with

$$D_c = D_z(1 + k_D c) \quad (6)$$

where D_z is a z-average translational diffusion coefficient and k_D the diffusion virial coefficient.

The extrapolation to zero concentration yields a diffusion coefficient D_z, which allows the calculation of the hydrodynamic radius R_h via the Stokes−Einstein law:

$$D_z = \frac{kT}{(6\pi\eta_0 R_h)}$$

Information about the inner structure of the scattering particles can be obtained from the so-called ρ ratio $\rho = R_G/R_h$.[17] ρ reflects the radial density distribution and is highly structure sensitive. Large values of ρ indicate open (i.e., rods) and low values rather dense structures (i.e., globular).

Viscosity Measurements. The viscosity measurements of the aqueous monomer solution were performed with an Ubbelohde cappillary viscosimeter.

Determination of Phase Diagram. Optical Polarizing Microscope. Binary mixtures of water and monomer or polymer were investigated by optical polarizing microscopy. We used a Leica DMRP microscope with a hot stage type Leitz 350 linked to a UKT 600 Lauda cryostate allowing temperatures down to −10 °C. The mixtures of water and surfactant were weighed in Teflon capsules with a stainless steel ball and homogenized in a vibration mill (Perkin-Elmer). Detection of phase transitions is always based on measurements with increasing temperature. An initial insight into the establishment of mesophases was obtained by penetration experiments,[18] which offer information over the whole concentration range, the temperature minima and maxima of the liquid crystalline and solid phases, the melting point, and lower and upper critical consolution points.

X-ray Diffraction. Samples were filled in glass tubes, sealed, and thermostated in a sample holder. The X-ray measurements were performed with a monochromatic Cu Kα ($\lambda = 1.54$ Å) beam, and a two-dimensional image plate system (700 × 700 pixels, 250 μm/125 μm resolution) was used as detector. The experimental setup allowed only measurements at $T \geq 20$ °C.

Results and Discussion

Characterization of Monomers and Polymers. The results of static and dynamic light scattering from dilute aqueous solutions of the monomers $EpEO_6C_X$ are summarized in Table 2. The measurements were performed in the range below 5 wt % monomer, where the concentration dependence of the viscosity followed Einstein's law. This indicates that in this range no concentration induced shape transition of the micelles occurs.

Both monomers exhibit a behavior which is rather common for nonionic surfactants. At low temperature small spherical micelles are found. Quasielastic light

Table 2. Results from Light Scattering of the Aqueous Monomer Solutions

	T, °C	M_W, g/mol	A_2, mol cm^3/g^2	R_{HS}, nm	D_Z, cm^2/s	R_h, nm	k_D, cm^3/g
$EpEO_6C_{10}$	15	37 000	2.53×10^{-4}	3.2	5.17×10^{-7}	3.3	7.072
	25	38 000	2.26×10^{-4}	3.2	6.93×10^{-7}	3.4	4.65
	35	41 000	2.03×10^{-4}	3.2	8.62×10^{-7}	3.7	4.301
$EpEO_6C_{12}$	15	59 000	9.13×10^{-5}	3.2	5.1×10^{-7}	3.7	−0.643
	25	60 000	9.45×10^{-5}	3.2	6.35×10^{-7}	3.9	−0.269
	35	236 000	6.44×10^{-5}	7.1	3.73×10^{-7}	8.5	3.529

Table 3. Results from Light Scattering of the Nonaqueous Polymer Solutions

	polymer				aggregate				
polymer	M_w, g/mol	R_G, nm	R_h, nm	ρ	M_w, g/mol	R_G, nm	R_h, nm	ρ	polymer per aggr
$PEpEO_6C_{10}$ 25 °C[a]	4.3×10^5	27	17	1.6	1.99×10^6	29	20	1.5	4.6
$PEpEO_6C_{10}$ 45 °C[a]	4.7×10^5	30	18	1.7	1.9×10^6	39	21	1.9	4
$PEpEO_6C_{12}$ I 25 °C[a]	3.6×10^6	33	21	1.6	11.8×10^6	72	36	2.0	3.3
$PEpEO_6C_{12}$ I 25 °C[b]					11.0×10^6	85	47	1.8	3.1[c]
$PEpEO_6C_{12}$ II 25 °C[b]	4.0×10^5	33	19	1.7	1.0×10^6	46	26	1.8	2.8
$PEpEO_6C_{12}$ II 45 °C[b]	3.6×10^5	33	23	1.4	9.6×10^5	46	28	1.6	2.7

[a] Isooctane. [b] Chloroform. [c] Calculated with M_w of the isooctane measurement.

scattering yields hydrodynamic radii of $R_h = 3.3$ nm ($X = 10$) and $R_h = 3.7$ nm ($X = 12$) (see Table 2). The respective equivalent thermodynamic hard sphere radius R_{HS} agrees reasonably well with these values. The aggregation numbers of 77 ($X = 10$) and 117 ($X = 12$) are rather close to that of the corresponding non-epoxy-modified surfactants hexaethylene glycol monodecyl ether $C_{10}E_6$ (73) and hexaethylene glycol monododecyl ether $C_{12}E_6$ (130).[19,20]

At higher temperature for the $X = 12$ system an increase of the molecular weigth M_W of the micelles and a decrease of A_2 is observed. The high molar mass of up to 236 000 g/mol is incompatible with a spherical micelle. The origin can be either an anisotropic growth of the spherical micelles to rod-or wormlike micelles,[20−22] an association of spherical micelles to random clusters,[23] or critical concentration fluctuations.[24]

The corresponding polymer surfactants are insoluble in water (see below). Light scattering measurements were, therefore, only possible in organic solutions. Due to the low refractive index increment dn/dc of the polymers in $CHCl_3$ and their low solubility in most conventional organic solvents, the light scattering experiments were performed in isooctane.

Vapor pressure osmometry identicated nearly no aggregation of the corresponding monomers in this solvent (only for the highest concentration investigated (160 g/L) trimers were observed.) Isooctane can, therefore, be expected to be a suitable solvent for the characterization of the properties of our polymeric surfactants.

For all polymer surfactants investigated, a minimum at about 2 g/L was observed in the concentration dependence of static light scattering. Figure 1 shows a typical Zimm diagram. Only the extrapolated values at zero scattering angle are plotted. The minimum was always located at about the same concentration, insensitive to variations of the measuring temperature, the length of the aliphatic tail group of the surfactant units, or the molecular weight of the polymer. The radius of gyration R_G exhibited a maximum and the diffusion coefficient a minimum at this concentration. This behavior is typical for a closed association, like micelle formation, where monomers aggregate up to a certain concentration.[25]

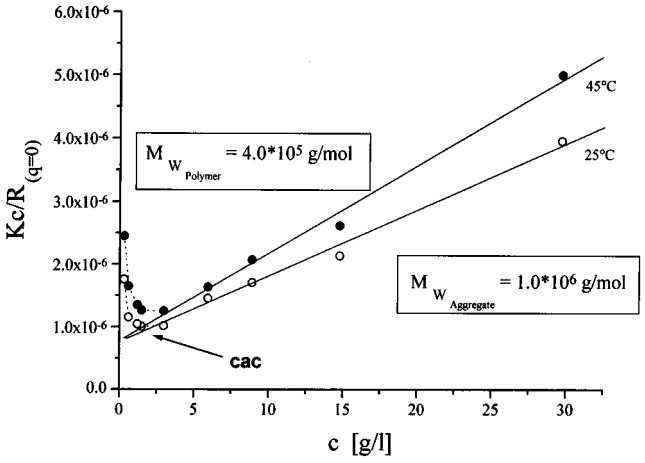

Figure 1. Concentration dependence of static light scattering at zero scattering angle from $PEpEO_6C_{12}$ II in isooctane at 25 °C (○) and 45 °C (●).

To obtain information about the single macromolecules measurements below $c = 2$ g/L were extrapolated, whereas extrapolation of the measurements at $c > 2$ g/L gives details about the aggregates. To increase the accuracy of the extrapolations the measurements have been repeated four times. The results were always identical within an error of ±10%. The results are summarized in Table 3.

With the samples $PEpEO_6C_{12}$, with the longer aliphatic tail at the monomeric units, aggregates of about three chains are formed (although the molecular weight of the single chains differs by a factor 10); with the shorter chain homologue $PEpEO_6C_{10}$ aggregates of about four are formed. Above the aggregation concentration the molar mass of the particles stayed stable and was found to be insensitive to temperature variation. A similar behavior was recently observed with a reversed-type polymer surfactant in water.[25]

The ρ-parameters (see Table 3) show values lying in the range of flexible chains; i.e., the single polymer

Table 4. Data of the Phase Behavior of Related Systems

substance		T_C	I_1	H_1	V_1	L_α	V_2	H_2
EO_6C_{10}[a]	*T*, °C	59		33		3		
	area, wt %			42−73		73−80		
$EpEO_6C_{10}$	*T*, °C	42		20				
	area, wt %			43−70				
$PEpEO_6C_{10}$	*T*, °C	26				28		11
	area, wt %					15−65		82−100
EO_6C_{12}[b]	*T*, °C	48		37	38	73		
	area, wt %			38−70	60−73	63−88		
$MeOEO_6C_{12}$[c]	*T*, °C	35		24	18	43		
	area, wt %			38−68	63−71	63−83		
$EpEO_6C_{12}$	*T*, °C	38				28		
	area, wt %					40−72		
$PEpEO_6C_{12}$	*T*, °C	44		21	29	44		32
	area, wt %			28−64	35−66	32−68		70−100

[a] Reference 27. [b] Reference 26. [c] Reference 18.

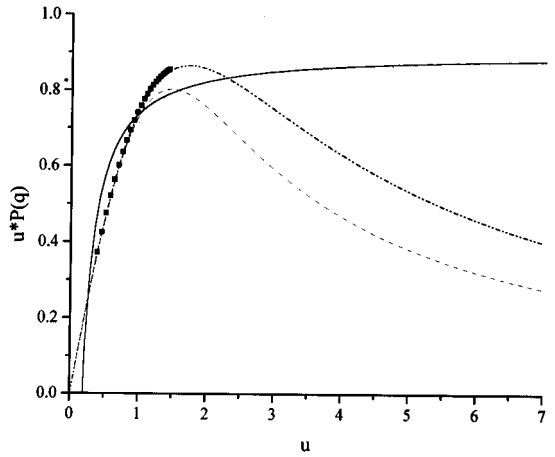

Figure 2. Casassa−Holtzer plot. Theoretical curves[17] for a monodisperse rigid rod (—), polydisperse coil (- ·· -), and monodisperse coil (- - -), and experimental data for $PEpEO_6C_{12}$ II (■).

molecules as well as the aggregates seem to adopt a random coil conformation.

Also an analysis of the particle scattering factor using a Casassa- Holtzer plot (see Figure 2) leads to this result. In Figure 2 is $uP(q)$ plotted against $u = qR_G$, for example, for polymer $PEpEO_6C_{12}$ II. For structural information only values for $u > 1$ are relevant.[17]

The data for all samples agree pretty well with the theoretical curves, calculated for polydisperse coils. The aggregation of several chains does, therefore, not lead to a pronounced stiffening of the backbone or even rodlike structures.

Phase Behavior. The phase diagrams of the monomeric $EpEO_6C_X$ systems with water (Figure 3 and 4) are similar to that of conventional oligooxyethylene alkyl ether amphiphiles.[26,27] The surfactants are soluble in water over the whole concentration range, despite the polymerizable epoxy groups located at their hydrophilic head.

They exhibit a high temperature miscibility gap typical for oligooxyethylene-based surfactants with a lower critical consolution point at $T_C = 42$ °C/5 wt % ($X = 10$) and $T_C = 38$ °C/5 wt % ($X = 12$); i.e., compared to the corresponding hydroxy-terminated surfactants $C_{10}E_6$ and $C_{12}E_6$, T_C is decreased by about 15 °C (see Table 4).

This can be explained by the fact that the epoxy group cannot form hydrogen bonds with the surrounding water to the same extend as the hydroxy group. A similar effect has been observed upon methyl substitution.[18]

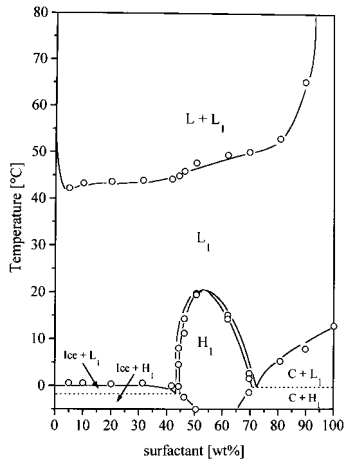

Figure 3. Phase diagram of $EpEO_6C_{10}$ in water.

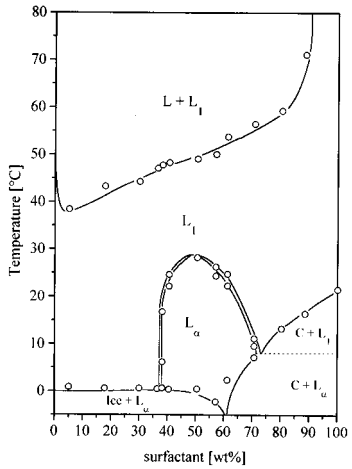

Figure 4. Phase diagram of $EpEO_6C_{12}$ in water.

Both surfactants exhibit only one liquid crystalline phase. For $X = 10$, a hexagonal liquid crystalline phase extends from 43 to 70 wt % with an upper temperature limit at 20 °C , which could be identified by a typical fanlike texture in the polarizing microscope. The fine grain mosaic texture of the $X = 12$ system corresponds to a lamellar phase ranging from 37 to 72 wt % with an upper temperature limit at 28 °C.

Polymerization of the epoxy group to the polymeric surfactant $PEpEO_6C_X$ has serious consequences for the phase behavior of the systems (Figures 5 and 6). In contrast to their corresponding monomers, the polymeric surfactants are not completely miscible with water, leading to a miscibility gap on the water rich side of

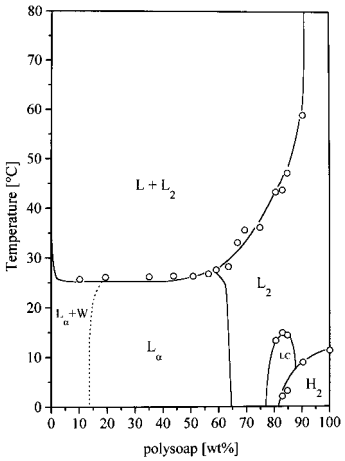

Figure 5. Phase diagram of $PEpEO_6C_{10}$ in water.

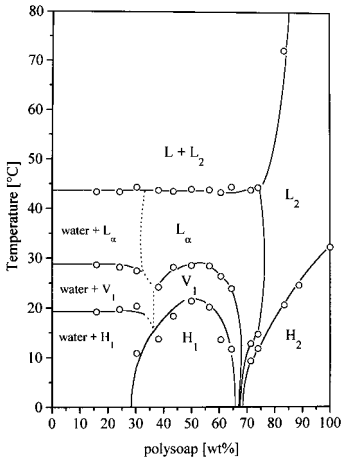

Figure 6. Phase diagram of $PEpEO_6C_{12}$ in water.

the phase diagram, which extends up to about 15 wt % ($X = 10$) or 28 wt % ($X = 12$) polysoap, respectively. This miscibility gap seems to be common to all headgroup fixed polysoap systems investigated up to now,[4,28] except for one system bearing very large and bulky hydrophilic heads.[29] For higher concentrations single phase areas including several mesophases were found, opposed to only one for the monomeric systems.

For $X = 10$ a lamellar liquid crystalline phase extends from 15 to 65 wt % with an upper temperature limit of 28 °C. The lamellar phase could be identified from the typical fine grain mosaic texture as well as from X-ray diffraction measurements, which yield reflections corresponding to layer spacings in the ratio $1:{}^1/_2:{}^1/_3$. An additional diffuse 0.45 nm spacing typical for liquid hydrocarbon chains[30] could be identified and is found in all our investigations. From 65 to 77 wt % exists a non-birefringent isotropic L_2 phase. In the range from 77 up to 90 wt % a birefringent phase could be identified with an upper temperature limit of 14 °C. This phase could not be specified, since it did not display a characteristic texture pattern. X-ray investigations failed due to thermostating problems (only temperatures above 20 °C were accessible). At high concentrations (>82 wt %) of the polymeric surfactant a hexagonal phase with an upper temperature limit of 11 °C occcurs. This phase exhibits the typical fanlike structure of hexagonal phases. From the sequence of mesophases follows that the observed hexagonal phase must be of the reversed type H_2.[31]

In the $X = 12$ system a normal type of hexagonal H_1, a cubic V_1, and a lamellar L_α phase exist in the region

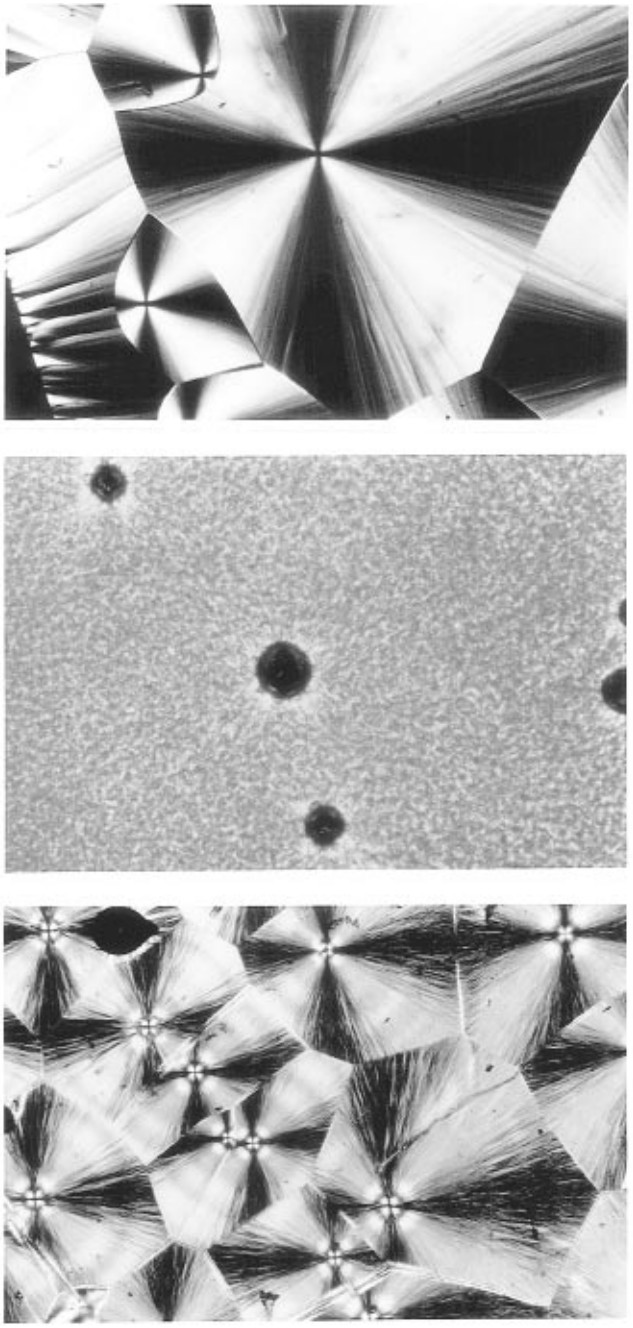

Figure 7. (a) Fanlike texture of the H_1 phase of $PEpEO_6C_{12}$. (b) L_α phase of $PEpEO_6C_{12}$. (c) Texture of the H_2 phase of $PEpEO_6C_{12}$.

from 30 to 69 wt %. All liquid crystalline phases show coexistence regions with the isotropic liquid in the lower concentration range. The upper temperature limits are 20 °C for the H_1, 29 °C for the V_1, and 44 °C for the L_α phase. The H_1 and L_α phase were recognized from their typical texture patterns (see Figure 7a,b). Additional X-ray investigations confirmed the typical $1:{}^1/_2:{}^1/_3$ reflection pattern of the lamellar phases. The V_1 phase is identified by its high viscosity, optical isotropy, and the transient birefringence observed upon shearing of the sample. In the concentration range above 69 wt % polymer a hexagonal phase exists, which could be identified by its typical fan like texture in a polarizing miscroscope (Figure 7c) as well as from the X-ray measurements. Reflexes corresponding to 6.22, 3.58, and 3.12 nm displayed the typical layer spacings in the ratio $1:1/3^{1/2}:1/4^{1/2}$. From the sequence of the meso-

phases it follows that the observed phase must be of the reversed H_2 type.

In comparison with the phase diagram of the monomeric, epoxy-teminated surfactant−water systems, the polymers exhibit a broader mesophase and a greater variety of different phases. This stabilization effect of liquid crystalline phases is well-known from other polysoap systems.

Interconnecting of individual surfactant molecules drastically slows down their mobility. Beyond this, attaching the surfactant units via their hydrohilic headgroup to a polymer backbone can be expected to lead to denser packing of surfactants along the polymer chain. This leads to a restricted freedom of conformations for the oligooxyethylene groups.This may be the origin of the lower solubility displayed by the miscibility gap at lower polymer concentrations.[4,32] The reduced headgroup area available per surfactant unit, due to the crowding along the polymer backbone, is probably reflected in the polymerization induced $H_1 \rightarrow L_\alpha$ transition observed in the $X = 10$ system. The occurence of a reversed hexagonal phase H_2 in both polymers investigated is to our knowledge the first example for the formation of a reversed liquid crystalline phase in side-chain polymeric surfactants. This indicates that a polymer backbone located at the hydrophilic end of the surfactant units is really able to stabilize reversed micelles, however, only if the polymer backbone and the hydrophilic headgroup are mutually compatible. This can be expected to be the case in our systems, where both are chemically identical.

Conclusion

The synthesized monomers display a behavior which is rather common for nonionic oligooxyethylene surfactants. They form spherical micelles in dilute aqueous solution. The introduction of the epoxy group to the hydrophilic head lowers the lower critical consolution point similar to the effect observed by methyl-terminated systems.[18] This effect is the result of a reduced possibility to form hydrogen bonds with surrounding water.

In contrast to the monomer, the corresponding polymeric surfactants form aggregates in apolar media like isooctane consisting of three or four single chains, respectively.

In water the polymers exhibit a miscibility gap in the low concentration regime typical for headgroup attached side-chain polymer surfactants. At higher concentrations several liquid crystalline phases can be observed. Due to the compatibility of the polymer backbone and the hydrophilic part of the side chains the formation of reversed aggregates is not disturbed. For the first time a reversed hexagonal H_2 phase in side-chain polymeric amphiphiles occurs.

Acknowledgment. We thank Prof. H.-F. Eicke for support of this work, H. Albrecht for help with the X-ray experiments, and H. Hammerich for viscosity measurements. We are grateful to the Swiss National Science Foundation for financial support of this work.

References and Notes

(1) Finkelmann, H. In *Polymer Liquid Crystals*; Ciferri, A., Kriegbaum, W. R., Meyer, R. B., Eds.; Academic Press: New York, 1982; p 35.
(2) Borisov, O. V.; Halperin, A. *Europhys. Lett.* **1996**, *34*, 657. Borisov, O. V.; Halperin, A. *Macromolecules* **1996**, *29*, 2612. Borisov, O. V.; Halperin, A. *Langmuir* **1995**, *11*, 2911.
(3) For example, see: Betton, F.; Theretz, A.; Elaissari, A.; Pichot, C. *Colloids Surf.* **1993**, *B1*, 97. Charreyre, M. T.; Boullanger, P.; Pichot, C.; Delair, T.; Mandrand, B.; Llauro, M. F. *Makromol. Chem.* **1993**, *194*, 117. Batz, H. G. *Adv. Polym. Sci.* **1977**, *23*, 25. Ferruti, P.; Danusso, F.; Franchi, G.; Polentarutti, N.; Garattini, S. *J. Med. Chem.* **1973**, *16*, 496. Pratten, M. K.; Lloyd, J. B.; Hörpel, G.; Ringsdorf, H. *Macromol. Chem.* **1985**, *186*, 725. Kiefer, M. Ph.D. Thesis, Freiburg, 1990. Pucci, B.; Polidori, A.; Rakotomanomana, N.; Chorro, M.; Pavia, A. A. *Tetrahedron Lett.* **1993**, *34*, 4185. Torstensson, M.; Hult, A. *Polym. Bull.* **1992**, *29*, 549. Schmidt, D. L.; Cobourn, C. E.; Dekoven, B. M.; Potter, G. E.; Meyers, G. F.; Fischer, D. A. *Nature* **1994**, *368*, 39.
(4) Laschewsky, A. *Adv. Polym. Sci.* **1995**, *124*, 1 and references cited herein.
(5) Lühmann, B.; Finkelmann, H.; Rehage, G. *Angew. Makromol. Chem.* **1984**, *123/124*, 217.
(6) Jahns, E.; Finkelmann, H. *Colloid Polym. Sci.* **1987**, *265*, 304.
(7) Weber, E. *Liebigs Ann. Chem.* **1983**, 770.
(8) Gingras, Bayley *Can. J. Chem.* **1957**, *35*, 599.
(9) Mulley, B. A. *J. Chem. Soc.* **1958**, 2065.
(10) Gibson, T. W. *J. Org. Chem.* **1980**, *45*, 1095.
(11) Emmons, W. D.; Pagano, A. S. *J. Am. Chem. Soc.* **1955**, *77*, 89.
(12) Vandenberg, E. A. *J. Polym. Sci.: Part A-1* **1969**, *7*, 525.
(13) Shih, J. S.; Tirrell, D. A. *J. Polym. Sci., Polym.Chem. Ed.* **1984**, *22*, 781.
(14) Muggee, J., Vogl, O. *J. Polym. Sci., Polym.Chem. Ed.* **1985**, *23*, 649.
(15) Andruzzi, F.; Lupinacci, D.; Magagnini, P. L. *Macromolecules* **1980**, *13*, 15.
(16) Yamakawa, H. In *Modern Theory of Polymer Solutions*; Harper & Row: New York, 1971.
(17) Burchard, W. In *Physical techniques for the study of food biopolymers*; Ross-Murphy, Ed.; Blackie Academic & Professional: Glasgow, 1994.
(18) Conroy , J. P.; Hall, C.; Leng, C. A.; Rendall, K.; Tiddy, G. J. T.; Walsh, J.; Lindblom, G. *Progr. Colloid Polym. Sci.* **1990**, *82*, 253.
(19) Degiorgio, V. In *Physics of Amphiphiles: Micelles, Vesicles and Microemulsions*; Degiorgio, V., Corti, M., Eds.; North-Holland Physics Publishing: Amesterdam, 1985; p 309.
(20) Brown, W.; Rymdén, R. *J. Phys. Chem.* **1987**, *91*, 3565.
(21) Kato, T.; Seimiya, T. *J. Phys. Chem.* **1986**, *90*, 3159.
(22) Medhage, B., Almgren, M.; Alsins, J. *J. Phys. Chem.* **1993**, *97*, 7753.
(23) Richtering, W. H.; Burchard, W.; Jahns, E.; Finkelmann, H. *J. Phys. Chem.* **1988**, *92*, 6032.
(24) Triolo, R.; Magid, L. J.; Johnson, J. S.; Child, H. R. *J. Phys. Chem.* **1982**, *86*, 3689. Strey, R.; Pakusch, A. *Surfactants Solution* **1987**, *4*, 465. Wilcoxon, J. P.; Schaefer, D. W.; Kaler, E. W. *J. Phys. Chem.* **1989**, *90*, 1909.
(25) Richtering, W.; Löffler, R.; Burchard, W. *Macromolecules* **1992**, *25*, 3642.
(26) Mitchell, D. J.; Tiddy, G. J. T.; Waring, L.; Bostock, T.; McDonald, M. P. *J. Chem. Soc. Faraday Trans. 1* **1983**, *79*, 975.
(27) Mulley, B. A.; Metcalf, A. D. *J. Colloid Sci.* **1964**, *19*, 501.
(28) Ferguson, P.; Sherrington, D. C.; Gough, A. *Polymer 1993*, *34*, 3291.
(29) Ito, K.; Tanaka, K.; Tanaka, H.; Imai, G.; Kawaguchi; S.; Itsuno, S. *Macromolecules* **1991**, *24*, 2348.
(30) Fontell, K. In *Liquid Crystals and Plastic Crystals: Physico-Chemical Properties and Methods of Investigation*; Gray, Winsor, Eds.; John Wiley & Sons: New York, 1974; p 80.
(31) Scriven, L. E. In *Mizellization, Solubilization and Microemulsions*; Mittal, K. L., Ed., Plenum Press: New York, 1977; Vol. 2, p 877.
(32) Hall, P. J.; Tiddy, G. J. T. In *Liquid Crystal Polymers From Structures to Applications*; Collyer, A. A., Ed.; Elsevier Science Publishers: Essex, 1992.

MA970410G